Characterization of Transient-Large-Amplitude Geomagnetic Perturbation Events

Brett A. McCuen[1], **Mark B. Moldwin**[1], **Mark Engebretson**[2]

[1]University of Michigan, Ann Arbor, Michigan
[2]Augsburg University, Minneapolis, Minnesota

Key Points:

- Short-timescale (< 60 s) geomagnetic perturbation events found at 6 high-latitude MACCS stations throughout 2015 are characterized.
- The existence of large-amplitude dB/dt at Earth's surface with timescale 1-10 seconds is demonstrated.
- The exact physical mechanisms driving TLA events are still unclear

Corresponding author: Brett A. McCuen, bmccuen@umich.edu

Abstract

We present a characterization of transient-large-amplitude (TLA) geomagnetic disturbances that occurred at six stations of the Magnetometer Array for Cusp and Cleft Studies throughout 2015. TLA events are defined as one or more short-timescale (< 60 seconds) dB/dt signature with magnitude ≥ 6 nT/s. A semi-automated dB/dt search algorithm was developed to identify TLA events in ground magnetometer data and used to identify 40 TLA dB/dt events. We demonstrate the existence of large-amplitude dB/dt with timescale less than 10 seconds in nine of the events. The association of these events to sudden commencements is relatively weak, rather the events are more likely to occur in relation to substorm onsets. However, 15% of TLA events show no direct association to geomagnetic storms, substorms or nighttime magnetic impulse events.

Plain Language Summary

Severe space weather events like geomagnetic storms and substorms cause geomagnetically induced currents (GIC) in electrically conducting material on Earth that are capable of damaging transformers and causing large-scale power grid failure. Models have been developed to forecast GIC that rely on estimation of the surface magnetic field fluctuations, dB/dt, but require knowledge of the geomagnetic field behavior on short-timescales (< 60 seconds) to more accurately predict GICs. Further, there is some evidence to suggest that extreme second-timescale geomagnetic perturbations may play a role in GIC production that has been previously overlooked. In this study, we investigate transient-large-amplitude (TLA) surface magnetic field disturbances in an effort to better understand the second-timescale nature of the geomagnetic field.

1 Introduction

Space weather events cause disturbances of the magnetosphere-ionosphere (M-I) system that result in fluctuations in the surface geomagnetic field. These large-amplitude surface magnetic perturbations, or dB/dt, generate geomagnetically induced currents (GIC) in electrical systems on Earth. GICs can be large enough to cause damage to transformers resulting in major power outages and costly equipment damage (Pulkkinen et al., 2017). The time derivative of the surface magnetic field, dB/dt, is often used to study GICs as it is proportional to the spatially-varying geoelectric field via Faraday's Law. In an effort to mitigate potential hazards and safeguard power systems, several models have been developed (e.g., Toth et al., 2005; Ngwira et al., 2014) to predict the geomagnetic behavior following severe space weather events. These models have been evaluated by their success in predicting whether the local horizontal dB/dt exceeds a threshold within a 20-minute time interval and have been validated by the geospace community (Pulkkinen et al., 2013).

However, there are still many challenges in accurately predicting dB/dt. Currently available models cannot predict minute or second-scale variation of the local magnetic field. An investigation of a method to improve the efficiency of the Space Weather Modeling Framework (SWMF) predictions by Toth et al, (2019) found that it is reasonably successful at predicting whether dB/dt will exceed some threshold in the next 20-minutes but it is unlikely that it would be successful in making this prediction in the next 5-minutes, ultimately concluding that 1-minute observed data are insufficient to accurately estimate dB/dt. While technological advancements in recent years have enabled surface magnetic field measurements with 1 s temporal resolution, geomagnetic perturbations in the $\sim$1 Hz frequency band have not been well studied due to their similarity to lightning signals whose impacts on technology are often well mitigated (e.g., Rivera er al., 2016; Gombosi et al., 2017), but analysis of transient-large-amplitude (TLA) geomagnetic disturbances could greatly improve space weather forecasting models.

In relation to GICs, second-scale dB/dt are generally attributed only to sudden commencements (SC) as an M-I driver (Kataoka & Ngwira, 2016). However, there is evidence to suggest that SCs are not the only driver for large-amplitude transient dB/dt at the surface. Several studies suggest that there are more complex, small-scale and localized processes involved in generating some extreme GICs (e.g., Engebretson et al., 2021; Ngwira et al., 2015, 2018). Further, a study by Simpson (2011) used a finite-difference time domain model to conclude that rapid ionospheric current fluctuations of order 1-second can induce substantial currents in power transmission lines following a severe coronal mass-ejection (CME).

Understanding the transient behavior of the surface geomagnetic field will help to improve GIC forecasting models to predict hazardous GICs more quickly and accurately, as well as enable a future investigation into whether large-amplitude, second-scale dB/dts play a role in producing GIC at the surface. In this study, we surveyed transient (<60 s), large-amplitude (> 6 nT/s) surface geomagnetic perturbation events that occurred at six stations of the Magnetometer Array for Cusp and Cleft Studies (MACCS) throughout 2015. We characterize these TLA signatures by their frequency of occurrence, temporal dependence and relation (or lack thereof) to various space weather events.

2 Data Set and Identification Technique

The data used in this study are from six ground magnetometer stations of the Magnetometer Array for Cusp and Cleft Studies (MACCS). The stations are located in northeast Nunavut, Canada, shown on the map in Figure 1 in corrected geomagnetic (CGM) coordinates (geographic and CGM coordinates are listed in Supporting Information Table S1). The CGM coordinates were calculated for the year of 2015 with the IGRF transformation tool of the World Data Center (WDC) for Geomagnetism, Kyoto. The MACCS magnetometers collect 8 samples per second in three axes, then averages and records the data at two samples per second (Hughes and Engebretson, 1997). The half-second sampling rate and high sensitivity (0.01 nT resolution) of the MACCS magnetometers is sufficient to detect shorter period Pc 1 and 2 pulsations. The geomagnetic variations measured by the magnetometers are in local geomagnetic coordinates: X (north-south), Y (east-west) and Z (vertical).

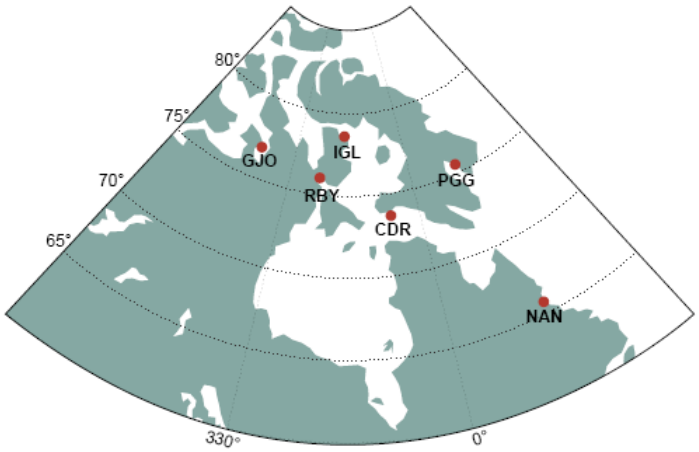

Figure 1: Map of the six MACCS stations used in this study with grid lines in corrected geomagnetic coordinates. Geographic and CGM coordinates for each station are listed in Table S1 in Supporting Information.

A semi-automated algorithm was developed to identify *dB/dt* signatures in magnetometer data with user-specified duration and magnitude. After initial data processing to remove instrument artifacts and smooth the data with a sliding average (if desired and with user-specified window length), the algorithm is essentially a series of filters. First the algorithm calculates the slope between each and every data point and determines the sign of the slope (assigns a 1 if positive slope, 0 if negative slope). If the sign of the slope changes for at least 1-second (two data points), the data point at which this change occurs (i.e. local minima or maxima) is flagged. Then the last filter recalculates the new *dB/dt* between each local maxima and minima and returns the information of the signature if it meets the conditions of the defined thresholds for dB/dt and Δt. The final product returned from the algorithm is a seven column matrix, each row represents an individual event and provides the start and end time of the event, start and end B value, the time elapsed of the event: *dt*, the change in magnetic field amplitude: *dB*, and finally the total perturbation: *dB/dt*.

We used this algorithm to identify *dB/dt* signatures with amplitude 6 nT/s or higher and duration less than 60 seconds. The *dB/dt* threshold is comparable to the surface magnetic field perturbations (approximately $\pm$8 nT/s) that caused the HydroQuebec power grid to fail during the geomagnetic storm of March 1989 (Kappenman, 2006). We characterize a transient-large-amplitude (TLA) *dB/dt* event as an occurrence of one or more of these signatures if they occur within 1-hour of another (regardless of the axis measured in and the station measured at). Because of the timescale and magnitude of the *dB/dt*s sought, many of these signatures are similar in nature to magnetometer noise caused either by instrumental artifacts or magnetic deviation due to by interference by ferromagnetic materials in the vicinity of the magnetometer (Nguyen et al., 2020). Thus, each event returned from the routine was visually inspected to confirm that it appeared to be of physical nature or remove it if it was a result of noise. In our manual inspection process, we found that the events resulting from magnetometer noise have several characteristics that make them possible to automatically detect. Our future work will incorporate a machine learning noise identification method that will help to fully automate the *dB/dt* search algorithm.

After the filtering process, a total of 181 transient-large-amplitude *dB/dt* signatures were identified. The majority ($\sim$63%) of these signatures were measured in the x-component, 29.5% in the y-component and 7.5% in the z-component. Finally, grouping the *dB/dt*s if they occurred within 1 hour of another signature resulted in a total of 40 TLA *dB/dt* events. While the primary temporal periods of interest in this study are 1-60 seconds, we also ran the algorithm with the upper limit for the duration of events extended to 5 minutes in order to compare to the 5-10 minute lasting magnetic impulse events (MIE) studied in Engebretson et al. (2019). Note that we used cleaned, full resolution half-second magnetic field data in this study and GIC measurement often involves averaging magnetometer data over 1 minute (e.g., Pulkkinen et al., 2006; Ngwira et al., 2008). Because our identification method relies on changes of the magnetic field lasting at least 1 second, some larger and more extended *dB/dt*s are undetected by our algorithm due to more rapid changes of the slope within.

Our analysis of TLA event dependence on space weather events relies on several databases. The SuperMAG Ring Current (SMR) index was used to determine geomagnetic storm activity and the SuperMAG Electrojet indices (SME) were used to examine auroral substorm activity during the events (supermag.jhuapl.edu/indices/). The association of TLA events with SCs was determined with the International Service of Geomagnetic Indices Sudden Commencement event list (isgi.unistra.fr/events_sc.php).

3 Occurrence of Transient-Large-Amplitude (TLA) *dB/dt* Events

We identified 40 TLA events consisting of one or more *dB/dt* signatures with magnitude 6 nT/s or higher and duration less than 60 seconds. Figure 2 shows three panels with examples of distinct TLA events identified at the MACCS stations in 2015. The hollow circles in all three panels of Figure 2 mark the start of each *dB/dt* within the TLA event and the solid dots mark the end. Note that axes in all plots of Figure 2 have been adjusted by subtracting the mean $B_{x,y,z}$ value from the interval, so the magnitude of the rate of change of the magnetic field is still to scale.

We expected to find many events occurring due to SCs as they have been considered the primary driver for the most rapid GICs (Kataoka & Ngwira, 2016). However, we found only one SC-related event, shown in Figure 2a. This is the only SC-related event despite five recorded SCs in 2015 that occurred when the MACCS stations were located on the dayside; the other four SCs caused *dB/dt*s at the MACCS stations that all lasted less than 60 seconds but did not exceed the 6 nT/s threshold. This TLA event started on 22 June 2015 at 18:33:22 UT (12:41:22 MLT, at RBY), just seconds after a large CME reached Earth causing an SSC at 18:33 UT. The largest *dB/dt* signature of the entire data set occurred in this event at RBY in the y-component, lasting 9.5 seconds with a magnitude of -33.49 nT/s. The *dB/dt*s measured in the y- and z-components at PGG and CDR all last 10.5 seconds or less, with the shortest event in the y-component at CDR with a magnitude of 13.3 nT/s and lasting just 5 seconds. All four stations were on the dayside during the time of the event.

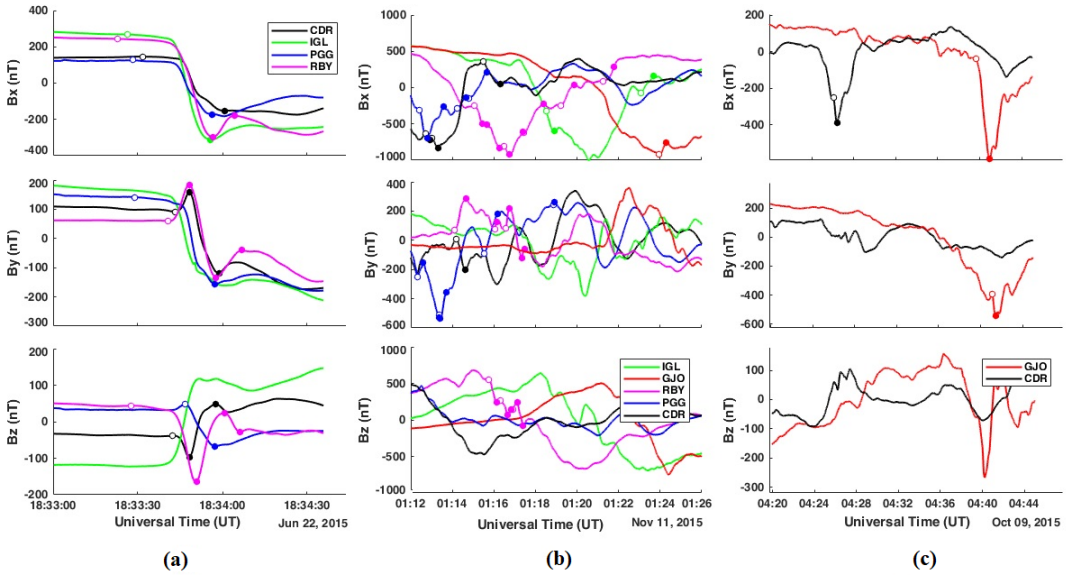

Figure 2: (a): A TLA event that occurred on 22 June 2015. (b): An event that occurred on 11 November 2015. (c) An event that occurred on 9 October 2015. All three panels show the x, y and z components of the surface magnetic field from top to bottom, respectively. Hollow circles mark the start of a dB/dt signature and the dots mark the end.

Shown in Figure 2b is an event that occurred on 11 November 2015 beginning at 01:12:20 UT (21:22:36 MLT of 10 November 2015). This event consists of 34 *dB/dt*s measured at all but the NAN station. Of these 34 *dB/dt*s, six have magnitude greater than 10 nT/s and five have duration < 10 seconds. One of the largest *dB/dt*s (16.2 nT/s) was measured at PGG at 1:13:21 UT in the y-component and lasted only 1 second. The over-

all event lasts about 10 minutes and occurs within a larger, longer (∼1 hour) magnetic impulse event (MIE) that is investigated by Engebretson et al. (2019). The MIE and the TLA event are not associated with a geomagnetic storm, although a substorm onset occurred at 01:07 UT, about 5 minutes prior to the start of the event. The MIE was preceded by a steady magnetic field for at least an hour prior to the start of the disturbance around 00:40 UT.

Finally, Figure 2c shows a TLA event on 9 October 2015 starting at 04:26:06 UT at the CDR station (23:31:06 MLT of 8 October 2015) where B_x decreases by 135.9 nT in 21 seconds (dB_x/dt = -6.46 nT/s). Then about 14 minutes later, two similar signatures occurred at GJO: a dB_x/dt of -6.87 nT/s at 04:49:37 UT and a dB_y/dt of -6.52 nT/s at 04:41:05 UT. Note, however, that the dB_x/dt at GJO actually lasted 80 seconds, this is one of the signatures identified when extending the upper threshold for the duration of the sample in the search algorithm to 5 minutes rather than 60 seconds. This TLA event occurred on the second day of recovery from a moderate geomagnetic storm (the SuperMAG Ring Current (SMR) index reached -123 nT in hour 23 of 7 October but recovered to around -34 nT during the hour of the event on 9 October) and there were marked substorm onsets occurring at 04:13 UT and 4:34 UT. Further, a nighttime MIE was identified at RBY at 04:37 UT but was not identified at CDR (note that GJO, the other station that measured this TLA event was not one of the stations used in the statistical study of Engebretson et al., 2019). There did occur a nighttime MIE measured at CDR later on at 22:00 UT of 9 October, and while no TLA signatures were identified at CDR during this time, a TLA event (dB_x/dt = -10.43 nT/s) was identified at PGG at 21:56:02 UT, preceding that MIE by several seconds.

We demonstrate the existence of significant magnetic disturbances with timescale $\leq$ 10 seconds in nine of the 40 TLA events identified. In five of these events, the shortest-timescale signatures exhibit the largest amplitude disturbances of the entire set of events ($|dB/dt| \geq$ 10 nT/s). Further, there are seven cases in which these signatures precede a larger, longer timescale (< 60 seconds) *dB/dt*. Examples of these signatures can be seen in Figure 2a (B_y at RBY: dB_y/dt = -33.49 nT/s), and in Figure 2b (the decrease in *By* at CDR at 18:33:43 UT lasts for 5 seconds and has rate of change of 13.23 nT/s; the two signatures in the z-component at CDR last 6 and 9.5 seconds with magnitudes of -9.85 and 15.28 nT/s, respectively).

4 Spatial and Temporal Characteristics and Space Weather Dependence

Of the 40 identified events, 27.5% consist of at least one *dB/dt* signature with magnitude exceeding 10 nT/s and half of these occurred within an event that has at least one other $|dB/dt| \geq$ 10 nT/s. These ten largest events were measured primarily between 73° and 76° CGM latitude at the PGG and CDR stations: PGG and CDR not only recorded the majority of the largest events but a substantial fraction (50% and 43%, respectively) of events in general. The GJO (76.86°) station recorded 9 events and RBY (75.62°) and IGL (78.63°) recorded 3 and 4 events, respectively. The southern-most station, NAN (65.67°), recorded just two events that were not recorded at any other station. In fact, 75% of the events were measured locally at only one station (the average, absolute distance from one station to the nearest station is ∼580 km. Note this average excludes NAN as it is the lowest latitude station with only two locally recorded events). Of the other 25% of events measured at more than one station, 4 were recorded relatively simultaneously (as shown in Figures 2a and 2b) while 6 other events had *dB/dt*s at more than one station delayed by at least 2 minutes (and at most 14 minutes, shown in Figure 2c).

TLA events occurred substantially more often in the Fall-Winter months with exactly 60% of events occurring in October through December. To illustrate the occurrence of TLA events as a function of magnetic local time as well as the association to geomag-

netic storms and substorms, Figure 3 shows the maximum *dB/dt* of each TLA event throughout 2015 as a function of MLT. The events that occurred between 18-6 MLT are plotted as squares with opacity according to temporal proximity of prior substorm onset: the black squares signify that the event started within 15 minutes after the nearest substorm onset and during nighttime hours of 18-6 MLT, the grey squares are events that occurred 15-30 minutes after substorm onset and the white squares occurred more than 30 minutes after the nearest substorm onset (daytime events were automatically marked as white squares). These onset delays were determined with the SuperMAG Newell and Gjerloev (2011) Substorm Event List (supermag.jhuapl.edu/substorms/). The bars extending from some of the squares in Figure 3 signify the full duration of the event if it consisted of multiple *dB/dt*s, showing at what point throughout the event that the maximum *dB/dt* occurred. Only three events occurred in the commencement or main phase of a geomagnetic storm, these are labeled in Figure 3. There are also five events that occurred on the first day of recovery from a geomagnetic storm and four events that occurred on the second day of recovery.

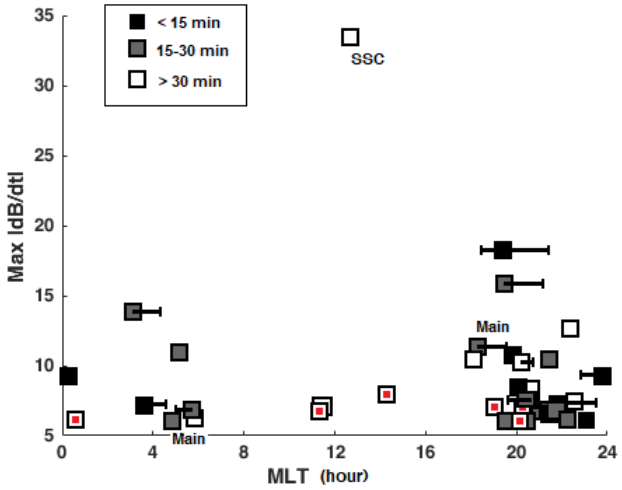

Figure 3: Maximum *dB/dt* as a function of magnetic local time (MLT) of each TLA event found in 2015. The bars extended from some squares signifies the duration of an event with multiple *dB/dt*s. The opacity of squares is based on the temporal proximity after the nearest substorm onset.

Figure 3 shows that a vast majority (90%) of events occur at nighttime between 18-6 MLT with peak number of events (70%) in the pre-midnight sector from 18-24 MLT. A large number of the events (65%) occurred within 30 minutes of substorm onset, but it is clear from Figure 3 that not all of the nighttime events show this association to substorm onsets (see white squares occurring at nighttime). While there is a strong association of TLA events to substorm onsets, 30% of events occurred more than 30 minutes after a substorm onset, with a small subset of events (6) that occurred more than 2 hours after substorm onset. Figure 3 also shows that the eleven *largest* TLA events ($\geq$ 10 nT/s) are more likely to occur between 18-24 MLT, but these are not necessarily more likely to occur within 30 minutes of substorm onset as about half of the set of largest events occurred more than 30 minutes after. As previously stated, five of these eleven largest events also have signatures lasting 10 seconds or less, with magnitude exceeding 10 nT/s. Comparison to the nighttime MIE events of Engebretson et al., (2019) found that 70% are related: either preceding the MIE within 30 minutes or occurring within the longer-timescale perturbation. Eight of the largest amplitude events were associated to a night-

time MIE. While the set of events exhibit a clear association to substorm activity and nighttime MIEs, there exists a subset of TLA events (15%) that occur more than 30 minutes prior to a nighttime MIE, more than 30 minutes after a substorm onset, and during relatively quiet geomagnetic conditions (i.e. not during any phase of a geomagnetic storm, nor occurring within two days of recovery), we classify these as unrelated events. These six events are expressed in Figure 3 as squares with red dots in the center. None of these unrelated events are in the set of largest disturbances, but they do show more temporal spread than the majority of events as two of these unrelated events are within the only four events that occurred during the daytime.

5 Discussion and Conclusions

While we identified a fairly small number of TLA events, the set exhibits several cases of large-amplitude ($\geq$ 10 nT/s) and very short-timescale ($\leq$ 10 s) disturbances. We found that SCs were not the main driver for these transient magnetic disturbances, although the large SSC that occurred on 22 June did cause the largest amplitude perturbation, it was the only TLA event associated to an SC despite many occurring over the course of the year. Rather, TLA *dB/dt*s occurred most often during local magnetic nighttime, with the highest frequency of events in the pre-midnight sector from 18-24 MLT. There is a clear association of these events to the onset of substorms as well as association to nighttime MIEs (about two-thirds occurring at nighttime within 30 minutes of substorm onset and about two-thirds related to MIEs), but there is not a perfect correlation between nighttime events and substorm-related events (i.e. not all nighttime events are substorm-related). Further, the relationship with substorm onsets appears to be a complicated one, as several events occurred multiple hours after the nearest substorm onset; this association will be investigated further in a future study extending the search for TLA events to many other stations and for a longer period of time.

In addition to a clear association to substorm onsets, we found that a majority of our events either preceded or occurred within a nighttime MIE (Engebretson et al., 2019). These nighttime MIEs are large-amplitude magnetic disturbances with 5-10 minute timescale occurring in this region of north-east Canada, the study surveyed MIEs from 2014-2017. Like MIEs, the TLA events identified were often but not always associated with substorms on a similar two-thirds basis. Using the spherical elementary current systems (SECS) method (Amm & Viljanen, 1999) and the implementation of this technique by Weygand et al. (2011), a superposed epoch analysis was conducted to investigate the average equivalent ionospheric currents (EIC) and inferred field-aligned currents (FAC) during 21 nighttime MIEs that occurred at CDR from mid-2014 to 2016. Engebretson et al. (2019a) found that the largest of these MIEs were associated to intense westward ionospheric currents 100 km above CDR, coinciding with a region of shear between upward and downward FAC. They also found that the largest horizontal *dB/dt*s occurred slightly south of CDR in a localized region of $\sim$275 km. Our TLA events show some similarities to these MIEs: 1) Of all six stations, the PGG and CDR stations measured the greatest number of events as well as the largest-amplitude events ($|dB/dt| \geq$10 nT/s) and 2) we found only nine events that were measured by more than one station, so the majority of our events ($\sim$75%) were measured locally at just one station. The localized nature of many TLA disturbances implies that the source currents are localized in the ionosphere (Boteler & Beek, 1999). More recent research has found extreme local enhancements of the geoelectric field with spatial scale $\sim$250-1600 km (Ngwira et al., 2015); these localized peak geoelectric fields occur during geomagnetic storms but the exact physical mechanism responsible for generating them is yet unknown. The TLA events studied in this paper are consistent with that of Ngwira et al. (2015), but also occur independent of geomagnetic storms (as well as auroral substorms and MIEs). Our future work will expand the data set to include more stations over an extended period of time and will include a superposed epoch analysis to investigate the ionospheric activity during TLA events.

In order to better understand our events in the context of these MIEs, we extended the upper threshold of the search algorithm to identify disturbances lasting up to 5 minutes with magnitude of 6 nT/s or greater. We found 25 additional *dB/dt*s that were all related to TLA events that we had already identified. Interestingly, only one signature lasted slightly longer than 2 minutes. We hypothesized that the absence of magnetic perturbations in the 2-5 minute timescale range could be due to algorithm bias. Because the method of the routine searches for changes in the direction of the slope (dB/dt) with the condition that the change last for at least 1 second and we used raw magnetic field data without any smoothing method, it was possible that the algorithm could be missing collections of dB/dt signatures lasting 2-5 minutes because there are shorter timescale variations occurring within them that did not meet the threshold of 6 nT/s. To test this theory, we applied a 10-point sliding average filter on the magnetic field data so that any of these shorter variations would be smoothed over, then ran the search algorithm for disturbances lasting up to 5 minutes again. Engebretson et al. (2019) also used a 10-point sliding average smoothing on the data. We found when the data were smoothed around 10-points, the algorithm identified all the same events as the raw data and identified 17 new events. All the events with signatures lasting > 60 seconds were the same apart from one case where the smoothed data marked the magnetic field response to the SSC at RBY as a disturbance lasting 60.5 seconds rather than 34 seconds. This occurred in many cases where the smoothed data identified the same signatures as longer e vents; because the algorithm searches for changes in the direction of the dB/dt, the 10-point smoothing was altering the exact moment that the slope changed sign and the signature started or ended. While the smoothing method resulted in many signatures marked as having longer duration, there was still only a small number of *dB/dt*s with > 1 minute timescale (32 as opposed to 25 with raw data) and the longest signature lasted 147 seconds. By comparing our results with smoothed data, we verified the methodology of the algorithm and determined that the absence of large-amplitude (≥ 6 nT/s) magnetic disturbances with timescale $\sim$2.5-5 minutes is not due to algorithm bias. This finding suggests that all longer-timescale magnetic perturbations at these stations consist of more rapid variations lasting less than 2.5 minutes, with a vast majority < 60 seconds.

While TLA events show a clear association with substorm activity as well as many shared characteristics with nighttime MIEs, TLA dB/dt events are not consistently related to these space weather events. We found a small subset of TLA events that are unrelated to geomagnetic storms, auroral substorms and nighttime MIEs. TLA events show a similar localized behavior with a weak association to geomagnetic storms, suggesting that there are other physical mechanisms, even beyond substorms, for localized peak enhancements in the geoelectric field (roughly proportional to the dB/dt). What we learned from the error analysis of this study is that a common smoothing method on the data altered the timing and amplitude of the events, suggesting that the short-timescale nature of the geomagnetic field could often be removed with common data processing methods or missed altogether with 1-minute or even 10-second averaged magnetic field data. Finally, we show that these signatures can have amplitude of the same order as longer-timescale events that are relevant to GICs. Our future work will include a statistical analysis on an expanded set of TLA events as well as an investigation of the geoelectric fields resulting from TLA dB/dt events in order to assess the potential threat they pose on technological infrastructure on Earth.

Acknowledgments

The tables of TLA events and space weather association information, as well as the algorithm developed for this research are available on the University of Michigan Deep Blue data repository (doi.org/10.7302/9t46-0092).

The authors thank the MACCS team for data (space.augsburg.edu/maccs/). MACCS is operated by the University of Michigan and Augsburg University and funded by the U.S. National Science Foundation via grants AGS-2013433 and AGS-2013648.

We gratefully acknowledge the SuperMAG collaborators (supermag.jhuapl.edu/info/?page=acknowledgement)

The results presented in this paper rely on the SC Event List calculated and made available by Observatori de L'Ebre, Spain from data collected at magnetic observatories. We thank the involved national institutes, the INTERMAGNET network and ISGI (isgi.unistra.fr).

References

Amm, O., & Viljanen, A. (1999). Ionospheric disturbance magnetic field continuation from the ground to the ionosphere using spherical elementary current systems. *Earth, Planets and Space*, *51*(6), 431–440. doi: 10.1186/BF03352247

Boteler, D. H., & Beek, G. J. V. (1999). August 4, 1972 revisted: A new look at the geomagnetic disturbance that caused the L4 cable system outage. *Geophysical Research Letters*, *26*(5), 577–580.

Boteler, D. H., Pirjola, R. J., & Nevanlinna, H. (1998). The effects of geomagnetic disturbances on electrical systems at the Earth's surface. *Advances in Space Research*, *22*(1), 17–27. doi: 10.1016/S0273-1177(97)01096-X

Engebretson, M. J., Hughes, W. J., Alford, J. L., Zesta, E., Cahill, L. J., Arnoldy, R. L., & Reeves, G. D. (1995). Magnetometer array for cusp and cleft studies observations of the spatial extent of broadband ULF magnetic pulsations at cusp/cleft latitudes. *Journal of Geophysical Research*, *100*(A10), 19371. doi: 10.1029/95ja00768

Engebretson, M. J., Pilipenko, V. A., Ahmed, L. Y., Posch, J. L., Steinmetz, E. S., Moldwin, M. B., ... Vorobev, A. V. (2019). Nighttime Magnetic Perturbation Events Observed in Arctic Canada: 1. Survey and Statistical Analysis. *Journal of Geophysical Research: Space Physics*, *124*(9), 7442–7458. doi: 10.1029/2019JA026794

Engebretson, M. J., Pilipenko, V. A., Steinmetz, E. S., & Moldwin, M. B. (2021). Nighttime magnetic perturbation events observed in Arctic Canada : 3 . Occurrence and amplitude as functions of magnetic latitude , local time , and magnetic disturbance indices.

Engebretson, M. J., Steinmetz, E. S., Posch, J. L., Pilipenko, V. A., Moldwin, M. B., Connors, M. G., ... Kistler, L. M. (2019). Nighttime Magnetic Perturbation Events Observed in Arctic Canada: 2. Multiple-Instrument Observations. *Journal of Geophysical Research: Space Physics*, *124*(9), 7459–7476. doi: 10.1029/2019JA026797

Gjerloev, J. W. (2012). The SuperMAG data processing technique. *Journal of Geophysical Research: Space Physics*, *117*(9), 1–19. doi: 10.1029/2012JA017683

Gombosi, T. I., Baker, D. N., Balogh, A., Erickson, P. J., Huba, J. D., & Lanzerotti, L. J. (2017). Anthropogenic Space Weather. *Space Science Reviews*, *212*(3-4), 985–1039. Retrieved from `http://dx.doi.org/10.1007/s11214-017-0357-5` doi: 10.1007/s11214-017-0357-5

Hughes, W., & Engebretson, M. (1997). MACCS: Magnetometer array for cusp and cleft studies. (1).

Kappenman, J. G. (2006). Great geomagnetic storms and extreme impulsive geomagnetic field disturbance events - An analysis of observational evidence including the great storm of May 1921. *Advances in Space Research*, *38*(2), 188–199. doi: 10.1016/j.asr.2005.08.055

Kataoka, R., & Ngwira, C. (2016). Extreme geomagnetically induced currents. , *3*(1). Retrieved from `http://dx.doi.org/10.1186/s40645-016-0101-x` doi:

10.1186/s40645-016-0101-x

Khomutov, S. Y., Mandrikova, O. V., Budilova, E. A., Arora, K., & Manjula, L. (2017). Noise in raw data from magnetic observatories. *Geoscientific Instrumentation, Methods and Data Systems*, *6*(2), 329–343. doi: 10.5194/gi-6-329-2017

Newell, P. T., & Gjerloev, J. W. (2011). Substorm and magnetosphere characteristic scales inferred from the SuperMAG auroral electrojet indices. *Journal of Geophysical Research: Space Physics*, *116*(12), 1–15. doi: 10.1029/2011JA016936

Newell, P. T., & Gjerloev, J. W. (2012). SuperMAG-based partial ring current indices. *Journal of Geophysical Research: Space Physics*, *117*(5), 1–15. doi: 10.1029/2012JA017586

Nguyen, N., Muller, P., & Collin, J. (2020). The Statistical Analysis of Noise in Triaxial Magnetometers and Calibration Procedure. *2019 16th Workshop on Positioning, Navigation and Communications (WPNC)*, 1–6. doi: 10.1109/wpnc47567.2019.8970255

Ngwira, C. M., Pulkkinen, A., Kuznetsova, M. M., & Glocer, A. (2014). Modeling extreme "carrington-type" space weather events using three-dimensional global MHD simulations. *Journal of Geophysical Research: Space Physics*, *119*(6), 4456–4474. doi: 10.1002/2013JA019661

Ngwira, C. M., Pulkkinen, A., McKinnell, L. A., & Cilliers, P. J. (2008). Improved modeling of geomagnetically induced currents in the South African power network. *Space Weather*, *6*(11). doi: 10.1029/2008SW000408

Ngwira, C. M., Pulkkinen, A. A., Bernabeu, E., Eichner, J., Viljanen, A., & Crowley, G. (2015). Characteristics of extreme geoelectric fields and their possible causes: Localized peak enhancements. *Geophysical Research Letters*, *42*(17), 6916–6921. doi: 10.1002/2015GL065061

Pulkkinen, A., Bernabeu, E., Thomson, A., Viljanen, A., Pirjola, R., Boteler, D., ... MacAlester, M. (2017). Geomagnetically induced currents: Science, engineering, and applications readiness. *Space Weather*, *15*(7), 828–856. doi: 10.1002/2016SW001501

Pulkkinen, A., Rastätter, L., Kuznetsova, M., Singer, H., Balch, C., Weimer, D., ... Weigel, R. (2013). Community-wide validation of geospace model ground magnetic field perturbation predictions to support model transition to operations. *Space Weather*, *11*(6), 369–385. doi: 10.1002/swe.20056

Pulkkinen, A., Viljanen, A., & Pirjola, R. (2006). Estimation of geomagnetically induced current levels from different input data. *Space Weather*, *4*(8). doi: 10.1029/2006SW000229

Rivera, M. K., Backhaus, S. N., Woodroffe, J. R., Henderson, M. G., Bos, R. J., Nelson, E. M., & Kelic, A. (2016). *Emp/gmd phase 0 report, a review of emp hazard environments and impacts* (Tech. Rep.). Retrieved from `http://permalink.lanl.gov/object/view?what=info:lanl-repo/lareport/LA-UR-16-28380` (Dataset: RASSTI)

Simpson, J. J. (2011). On the possibility of high-level transient coronal mass ejection-induced ionospheric current coupling to electric power grids. *Journal of Geophysical Research: Space Physics*, *116*(11), 1–12. doi: 10.1029/2011JA016830

Tóth, G., Sokolov, I. V., Gombosi, T. I., Chesney, D. R., Clauer, C. R., De Zeeuw, D. L., ... Kóta, J. (2005). Space weather modeling framework: A new tool for the space science community. *Journal of Geophysical Research: Space Physics*, *110*(A12), 1–21. doi: 10.1029/2005JA011126

Weygand, J. M., Amm, O., Viljanen, A., Angelopoulos, V., Murr, D., Engebretson, M. J., ... Mann, I. (2011). Application and validation of the spherical elementary currents systems technique for deriving ionospheric equivalent currents with the North American and Greenland ground magnetometer arrays. *Journal of Geophysical Research: Space Physics*, *116*(3), 1–8. doi:

10.1029/2010JA016177

Figure 1.

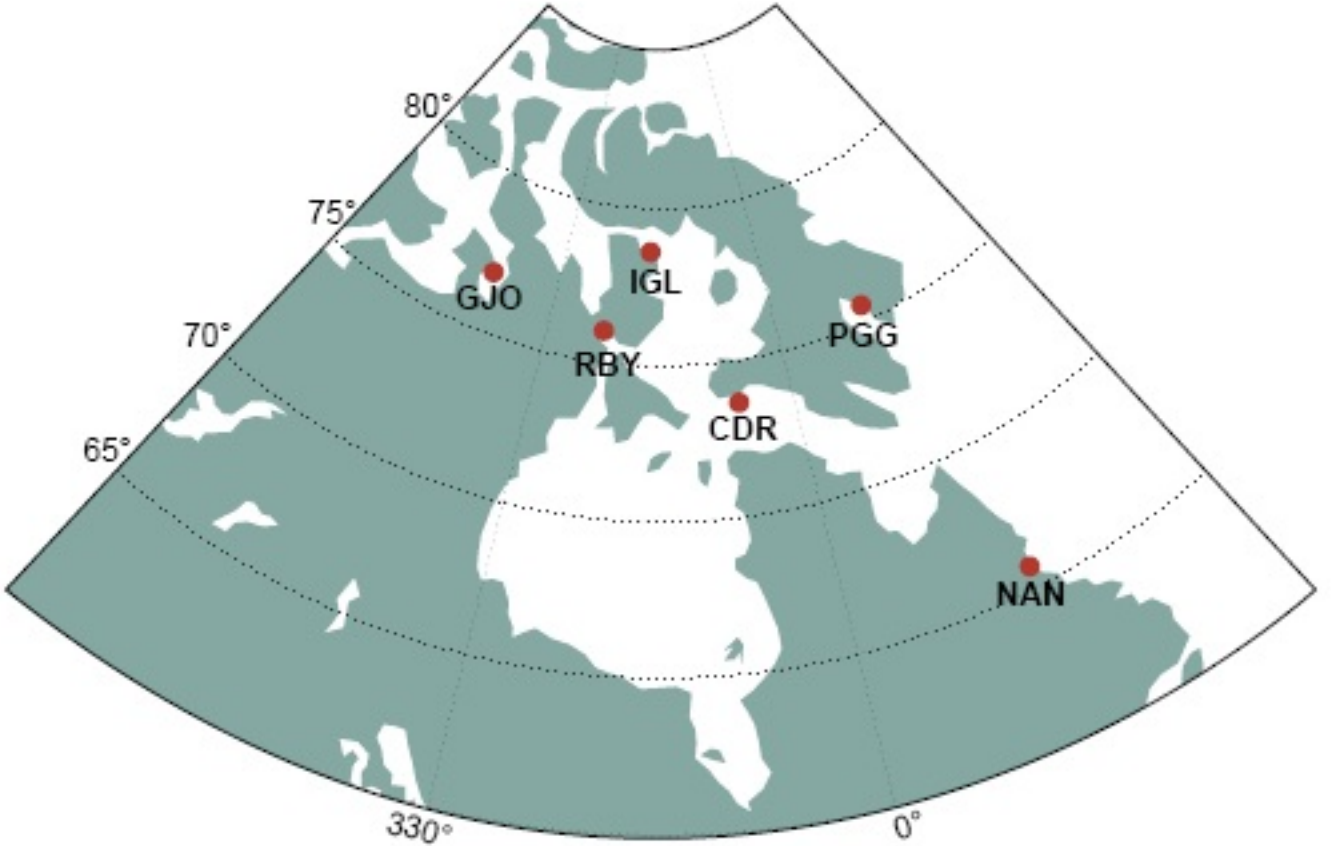
80°
75°
70°
65°
330°
0°
GJO
IGL
RBY
PGG
CDR
NAN

Figure 2.

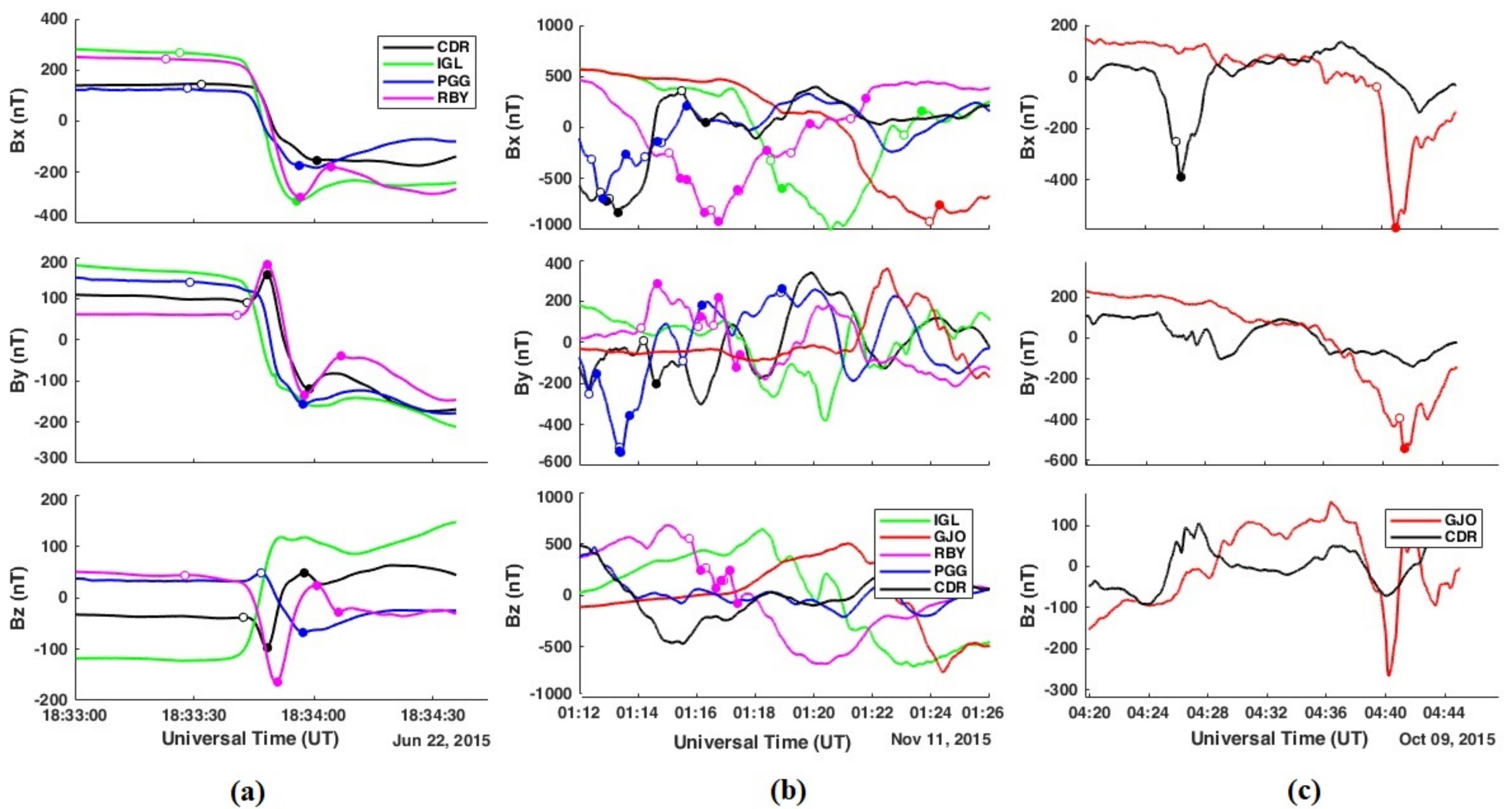
Bx (nT)
By (nT)
Bz (nT)
CDR
IGL
PGG
RBY
GJO
18:33:00
18:33:30
18:34:00
18:34:30
Universal Time (UT)
Jun 22, 2015
01:12
01:14
01:16
01:18
01:20
01:22
01:24
01:26
Nov 11, 2015
04:20
04:24
04:28
04:32
04:36
04:40
04:44
Oct 09, 2015
(a)
(b)
(c)

Figure 3.

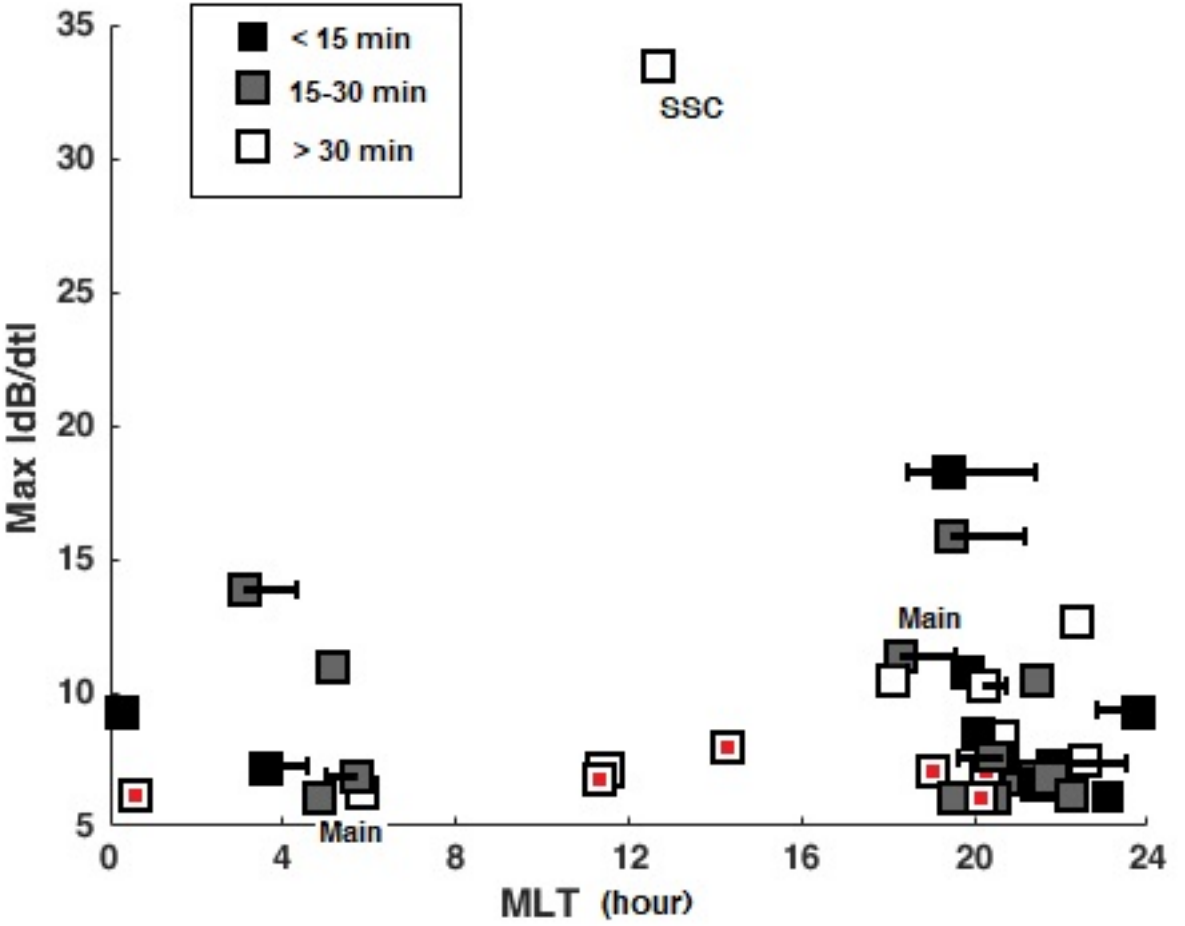
< 15 min
15-30 min
> 30 min
SSC
Main
Main
Max |dB/dt|
MLT (hour)
35
30
25
20
15
10
5
0
4
8
12
16
20
24